

Driven Bose-Hubbard Model with a Parametrically Modulated Harmonic Trap

N. Mann¹, M. Reza Bakhtiari¹, F. Massel², A. Pelster³ and M. Thorwart^{1,4}

¹*I. Institut für Theoretische Physik, Universität Hamburg, Jungiusstraße 9, 20355 Hamburg, Germany*

²*Department of Physics and Nanoscience Center, University of Jyväskylä,
P.O. Box 35 (YFL), FI-40014 University of Jyväskylä, Finland*

³*Physics Department and Research Center OPTIMAS, Technical University of Kaiserslautern,
Erwin-Schrödinger Straße 46, 67663 Kaiserslautern, Germany*

⁴*The Hamburg Centre for Ultrafast Imaging, Luruper Chaussee 149, 22761 Hamburg, Germany*

We investigate a one-dimensional Bose-Hubbard model in a parametrically driven global harmonic trap. The delicate interplay of both the local atom interaction and the global driving allows to control the dynamical stability of the trapped quantum many-body state. The mechanism is illustrated for weak interaction by a discretized Gross-Pitaevskii equation within a Gaussian variational ansatz, yielding to a Mathieu equation for the condensate width. The parametric resonance condition can be tuned by the atom interaction strength. For stronger interaction, this mechanism is confirmed by results of the numerically exact time-evolving block decimation scheme. The global modulation also induces an effective time-independent inhomogeneous hopping strength for the atoms.

Strong external time-dependent driving is known to have pronounced implications for quantum many-body systems [1]. For instance, light can induce a collapse of long-range ordered charge-density-wave phases [2–5], deconstruct insulating phases [6–8], break Cooper pairs [9–12], or induce novel transient superconducting phases [13–19]. An interesting class of externally driven systems are parametric oscillators in which the characteristic frequency is periodically modulated. Already the classical Kapitza pendulum is known for its peculiar dynamics [20] which is stabilized by properly choosing the driving parameters. The parametric quantum harmonic oscillator has even a nonlinear Floquet spectrum [21, 22] with regimes of stable and unstable quantum dynamics.

Novel concepts of driven quantum many-body systems can be studied in atomic quantum gases [23–26]. For instance, a periodically modulated atomic interaction can stabilize a Bose-Einstein condensate [27–29]. Moreover, the superfluid-Mott insulator transition can be controlled [30–33] or novel synthetic quantum matter [34] can be realized by Floquet engineering [35, 36]. Also, anyonic statistics [37] might be accessible [38]. Local modulations can coherently control the single-particle tunneling in shaken lattices [39], magnetic frustration [40], and effective magnetic fields [41]. Modulated local onsite Bose-Hubbard interactions can lead to correlated tunneling [42] and artificial gauge potentials, and thus to novel topological phases [43]. All these works commonly rely on the time-periodic modulation of *local* parameters.

Crucial for externally driven quantum many-body systems is the interplay of the atomic short-range interaction and the external driving. When a system is driven parametrically, it exchanges energy with the driving field, and in principle can be heated to infinite temperature [44, 45]. On the other hand, the parametric oscillator has regions of dynamical stability as well. So the natural question arises how does the atomic interaction affect the stability of a globally parametrically driven quantum

many-body system. Can short-range interaction stabilize a quantum gas in a parametric trap which would otherwise be unstable? In turn, can we obtain information on the atomic interaction by externally tuning the system to an unstable dynamical state?

In this Letter, we show that a *global* parametric modulation of the trapping potential, which does not have to be tuned to local properties, can be used to control the stability of the interacting quantum gas. In particular, the global condensate dynamics in a parametrically modulated trap can be stabilized or destabilized by tuning the atomic interaction strength. Conversely, locating the onset of the instability can be used to determine the atom interaction strength. To illustrate the mechanism, we investigate the parametrically driven Bose-Hubbard model with repulsive interaction. The effect is apparent already on the level of a mean-field Gross-Pitaevskii ansatz for the condensate wave function and is supported by a numerically exact treatment in terms of the time-evolving block-decimation (TEBD) method.

Model – We consider a one-dimensional Bose-Hubbard model with a global harmonic potential with a time-dependent curvature $V(t) = V_0 + \delta V \sin \Omega t$. The potential has a time-averaged curvature V_0 , which is parametrically modulated with the strength δV and the frequency Ω . The model Hamiltonian reads with $\hbar = 1$

$$H(t) = -J \sum_{\ell} \left(b_{\ell}^{\dagger} b_{\ell+1} + \text{h.c.} \right) + \frac{U}{2} \sum_{\ell} n_{\ell} (n_{\ell} - 1) + V(t) \sum_{\ell} (\ell - \ell_0)^2 n_{\ell}, \quad (1)$$

where J is the hopping amplitude and U the on-site interaction strength. Furthermore, $b_{\ell} (b_{\ell}^{\dagger})$ are the bosonic annihilation (creation) operators at site ℓ , and $n_{\ell} = b_{\ell}^{\dagger} b_{\ell}$ denotes the local occupation number operator. We consider a lattice with M sites loaded with N bosonic atoms. Thus, the lattice center is located at $\ell_0 = (M - 1)/2$.

Quantum many-body parametric resonance – In the non-interacting limit $U = 0$ and for no driving, the system can be mapped exactly to a discretized quantum harmonic oscillator with frequency $\omega_0 = 2\sqrt{JV_0}$ and unity mass with a Gaussian ground state. When the parametric driving is switched on, the parametric resonance at $n\Omega = 2\omega_0$ produces regions of instability in the parameter space [21, 22] with diverging position and momentum variances. The driven single-particle problem is still exactly solvable in terms of the Mathieu equation with its known stability diagram. For interacting particles, this is no longer possible. To elucidate the impact of quantum many-body interactions on the parametric resonance, we first consider a dilute, weakly interacting atom gas at zero temperature with the mean-field Lagrangian density

$$L = \frac{1}{N} \sum_{\ell} \left[\frac{i}{2} (\psi_{\ell}^* \partial_t \psi_{\ell} - \psi_{\ell} \partial_t \psi_{\ell}^*) + J(\psi_{\ell}^* \psi_{\ell+1} + \text{h.c.}) - V(t)(\ell - \ell_0)^2 \psi_{\ell}^* \psi_{\ell} - \frac{U}{2} \psi_{\ell}^* \psi_{\ell}^* \psi_{\ell} \psi_{\ell} \right], \quad (2)$$

obtained from the Hamiltonian (1), with the mean-field condensate wave function $|\psi\rangle = \sum_{\ell} \psi_{\ell} b_{\ell}^{\dagger} |0\rangle$. By extremizing the Lagrangian with respect to $\psi_{\ell}(\psi_{\ell}^*)$, one arrives at a discretized version of the Gross-Pitaevskii equation. To obtain the time evolution of the boson gas, we use a Gaussian trial wave function [46]

$$\psi_{\ell} = \left(\frac{N^2}{\pi \alpha^2} \right)^{1/4} \exp \left[-\frac{(\ell - \ell_0)^2}{2\alpha^2} + i\beta(\ell - \ell_0)^2 \right], \quad (3)$$

with a time-dependent width $\alpha \equiv \alpha(t)$ and $\beta \equiv \beta(t)$ and minimize L with respect to α and β .

In the following, we consider the regime $J \gg V_0$, where the condensate is extended over many sites, i.e., $\alpha \gg 1$. Then, all sums over ℓ can be approximated by continuous integrals and the Lagrangian takes the form

$$L = 2J e^{-\frac{1}{4\alpha^2} - \beta^2 \alpha^2} - \left[\dot{\beta} + V(t) \right] \frac{\alpha^2}{2} - \frac{UN}{2\sqrt{2\pi}\alpha}. \quad (4)$$

The Euler-Lagrange equations $\partial_x L = \frac{d}{dt} \partial_{\dot{x}} L$ for $x = \alpha, \beta$ provide the equations of motion $\dot{\alpha} = 4J_{\gamma} \alpha \beta$ and

$$\ddot{\alpha} + \dot{\gamma} \dot{\alpha} + 4J_{\gamma} V(t) \alpha = \frac{4J_{\gamma}^2}{\alpha^3} + \frac{2J_{\gamma} UN}{\sqrt{2\pi}\alpha^2}, \quad (5)$$

with $\gamma = \frac{1}{4\alpha^2} + \alpha^2 \beta^2$ and $J_{\gamma} = J e^{-\gamma}$.

Aiming at a stability analysis, we expand the width $\alpha(t) = \alpha_0 + \delta\alpha(t)$ in terms of small deviations from its equilibrium value α_0 with $\alpha_0 \gg |\delta\alpha(t)|$, and linearize Eq. (5) with respect to $\delta\alpha$. Taking into account correspondingly $\beta(t) = \beta_0 + \delta\beta(t)$ with $\beta_0 = 0$ we find that the stationary solution α_0 follows implicitly from $2V_0\alpha_0^4 = 2J e^{-1/4\alpha_0^2} + UN\alpha_0/\sqrt{2\pi}$ and that the deviation $\delta\alpha$ from equilibrium obeys

$$\delta\ddot{\alpha} + 4J' [V' + \delta V' \sin \Omega t] \delta\alpha = -4J' \delta V \alpha_0 \sin \Omega t, \quad (6)$$

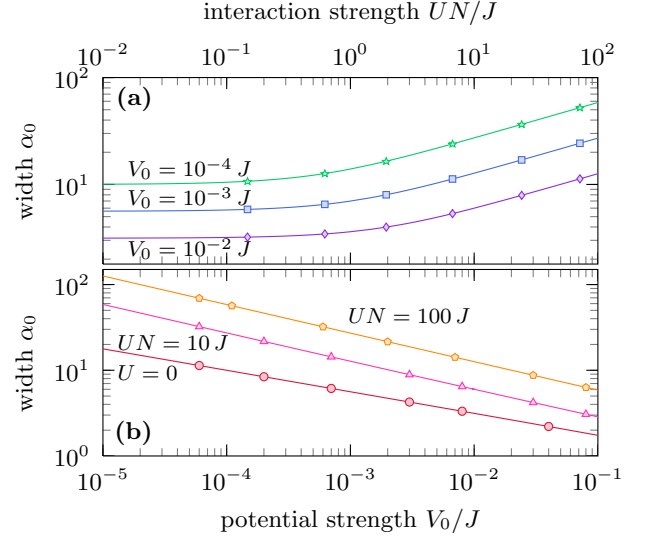


FIG. 1. Stationary condensate width α_0 (within the mean-field picture) as function of (a) interaction strength UN for different potential curvatures V_0 , and (b) V_0 for different UN .

where both the hopping $J' = J e^{-1/4\alpha_0^2}$ and the driving strength $\delta V' = \delta V(1 + 1/2\alpha_0^2)$ are renormalized. Further, the atomic interaction renormalizes the potential curvature such that

$$V' = V_0 \left(1 + \frac{1}{2\alpha_0^2} \right) + \frac{J'}{\alpha_0^4} \left(3 - \frac{1}{\alpha_0^2} \right) + \frac{UN}{\sqrt{2\pi}\alpha_0^3} \left(1 - \frac{1}{4\alpha_0^2} \right). \quad (7)$$

It ranges from $V' \simeq 4V_0$ in the non-interacting limit to $V' \simeq 3V_0$ in the Thomas-Fermi limit, i.e., when the kinetic term can be neglected. Equation (6) is the well-known Mathieu equation with an additional time-dependent force term. This inhomogeneity does not influence the parametric resonance [29]. Thus, for $\delta V' \ll V'$, $\delta\alpha(t)$ exhibits a resonant behavior when the parametric resonance condition $n\Omega = 2\omega'$ with the resonance frequency $\omega' = 2\sqrt{J'V'}$ is fulfilled for $n = 1, 2, \dots$

In Fig. 1 a), we show the stationary condensate width α_0 as a function of the interaction strength for different potential curvatures. Below $UN \lesssim J$, the condensate width $\alpha_0 \simeq (J/V_0)^{1/4}$ is mainly determined by the potential curvature V_0 and only gradually increases with UN . For $UN > J$, the U -term becomes comparable in size to the J -term which leads to a steeper growth of α_0 . In fact, the condensate width behaves as $\alpha_0 \sim U^{1/3}$ in the Thomas-Fermi limit. Moreover, in Fig. 1 b), we show the condensate width α_0 as a function of the static potential curvature V_0 . In all cases, we find an algebraic decrease of $\alpha_0 \sim V_0^{-1/\eta}$ with increasing V_0 , where $3 \leq \eta \leq 4$. In the non-interacting limit we find $\eta = 4$, whereas in the strongly interacting limit we obtain $\eta = 3$.

The resonance frequency ω' is also modified by the condensate interaction. In Fig. 2 (main), we depict the

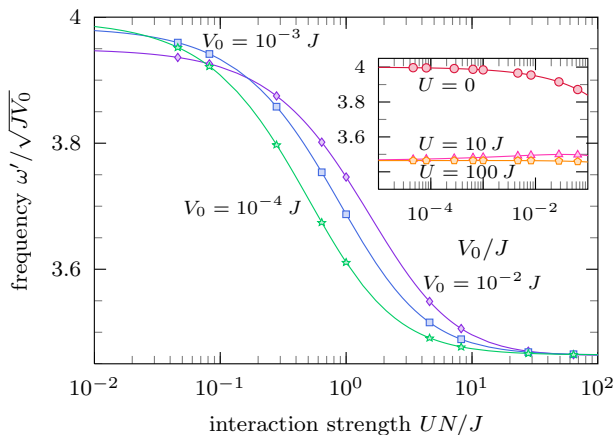


FIG. 2. Resonance frequency ω' as function of UN for different V_0 (main) and in dependence of V_0 for different UN (inset).

dependence of ω' on the interaction strength for various potential curvatures. For ease of comparison, we show the resonance frequency scaled to $\sqrt{JV_0} = \omega_0/2$. For strong interaction $U \gg J/N$, the resonance frequency turns out to be independent of the interaction U and approaches $\omega' = 2\sqrt{3JV_0}$, where $J \simeq J'$ is satisfied. In the opposite limit of non-interacting bosons, $J = J'$ is not satisfied per se. This is especially the case for a steep potential when V_0 is so large that α_0 is only of the order of several lattice sites. In this regime, the resonance frequency is given by $\omega' = 4\sqrt{JV_0}\sqrt{1 + 1/(2\alpha_0^2)}e^{-1/8\alpha_0^2}$. In the inset of Fig. 2, we show the resonance frequency as a function of the potential curvature for different interaction strengths. For a small (large) enough interaction strength U the resonance frequency ω' weakly decreases (increases) with the potential steepness V_0 .

Next, we address the condensate stability in the parametrically modulated trap. To get information about the onset of the parametric instability on a general basis, we write Eq. (6) in terms of two coupled first-order linear differential equations. By using the Floquet theorem [47], we determine whether the solutions for a given set of parameters are stable or not [48]. In Fig. 3, we show the resulting stability diagram as a function of the interaction strength UN and the driving strength δV for a fixed potential curvature V_0 and three different values of the driving frequency Ω . Each curve divides the parameter space into regions with stable or unstable behavior of the condensate. In the region below each curve, all solutions of Eq. (6) are stable, while in the region above, at least one solution is unstable. At resonance, i.e., $n\Omega = 2\omega' = 4\sqrt{JV'}$, an infinitesimally small driving amplitude is sufficient to destabilize the condensate entirely. A finite particle interaction may cause a transition from a stable to an unstable behavior. Hence, atom-

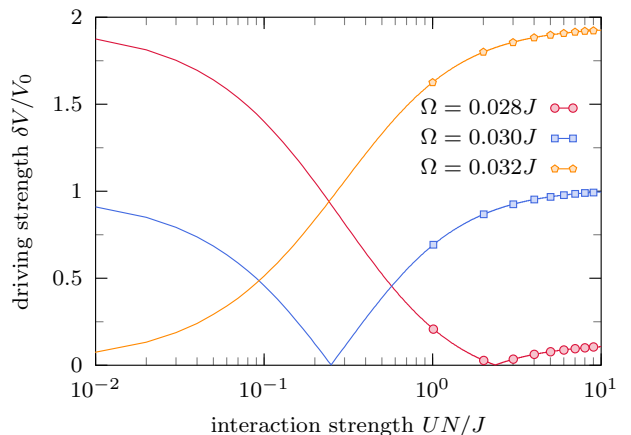


FIG. 3. Stability diagram of parametrically driven BEC for the first resonance $n = 1$. Horizontal axis indicates the particle interaction UN and vertical axis the parametric driving strength δV for $V_0 = 1.6 \times 10^{-5} J$ for different driving frequencies Ω as indicated. Unstable (stable) solutions exist in the regions above (below) each curve.

atom interaction may be explored to stabilize a condensate in a parametrically modulated trap by modifying the resonance condition. Moreover, the onset of the parametric instability can be used to measure the interaction strength.

Transient dynamics beyond the mean-field approach – Next, we determine the quantum many-body dynamics of a strongly interacting gas in a parametrically driven trap numerically exactly by using the TEBD [49–51]. Although it is still impossible to reach asymptotic times, we obtain the numerically exact transient dynamics and are able to detect the onset of the parametric resonance and the instability.

First, we consider the static case $\delta V = 0$ and calculate the ground state of the Hamiltonian Eq. (1). Then, the condensate width is extracted as the full width at half maximum (FWHM) of the distribution of the local occupation number $\langle n_\ell \rangle$ [52]. We use a lattice with $M = 32$ sites filled with $N = 16$ bosons in a trap with $V_0 = 0.0922 J$. In Fig. 4, we show the condensate width in dependence of U calculated numerically exactly in comparison to the mean-field result α_0 . The inset depicts the corresponding distribution $\langle n_\ell \rangle$. A perfect agreement is found for $U = 0$, where both approaches yield coinciding Gaussians. Deviations between the two results increase for growing U as expected. For $U = 7 J$, a plateau-like Mott region with a nearly integer occupation number starts to appear in the numerical result, see inset of Fig. 4. This wedding-cake-like structure cannot be reproduced by the variational mean-field approach. The reasons for the deviations are twofold. Beyond finite size effects in the numerically exact result, for increasing U , the condensate starts to locally form a Mott insulat-

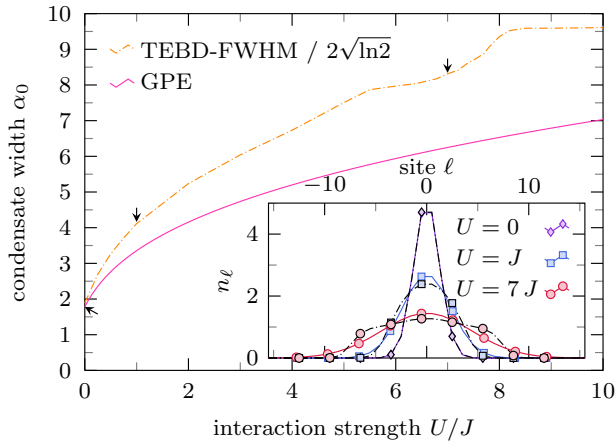


FIG. 4. Comparison of condensate width determined by the numerically exact FWHM (TEBD, dashed line) and variational mean-field result α_0 (GPE, solid line) for a half-filled lattice of $M = 32$ sites. The curvature of the trapping potential is set to $V_0 = 0.0922 J$ and $\delta V = 0$. The step refers to the Berezinsky-Kosterlitz-Thouless quantum phase transition (see text). Inset: Local occupation number $\langle n_\ell \rangle$ ($\psi_\ell^* \psi_\ell$) for $U = 0$ (diamond), $U = J$ (square) and $U = 7J$ (circle) for the same V_0 (dashed lines: TEBD, solid lines: GPE).

ing state. The quantum fluctuations at larger U become increasingly important and lead to a broadening of the population density. This is not taken into account by the GPE mean-field approach, but is captured by the TEBD. In fact, for all U , the condensate width is systematically larger than predicted by the mean-field approach. Interesting is the step-like increase of the condensate FWHM at $U \approx 7J$ which accompanies the formation of the Mott plateau. In fact, this is a signature of the Berezinsky-Kosterlitz-Thouless quantum phase transition which has been shown to occur between $U = 7.5 J$ and $U = 8 J$ for the $n = 1$ Mott lobe [53, 54].

Having studied the static trap, we next address the transient dynamics of the parametrically driven trap. At initial time $t = 0$, we prepare the system in the ground state of the Hamiltonian $H(0)$. In Fig. 5 a), we show the time evolution of the total energy $\Delta E(t) = E(t) - E(0)$ as a function of time t and driving frequency Ω with $E(t) = \langle H(t) \rangle$. In Fig. 5 b), we show two cuts along the lines $\Omega = 1.31 \omega'$ and $\Omega = 2.34 \omega'$. The resonance frequency ω' can be estimated according to Eq. (2). Resonant driving in Fig. 5 is expected to occur close to $\Omega/\omega' = 2/n$. We find clear evidence of the two-photon resonance $n = 2$ which is manifest in a growth of the total energy after each period. The resonance is slightly shifted to $\Omega \simeq 1.3 \omega'$, due to the strong interaction between the atoms which is not taken into account in the variational mean-field description. However, the $n = 1$ resonance is not observed in the transient dynamics and is expected to occur at longer times. For off-resonant

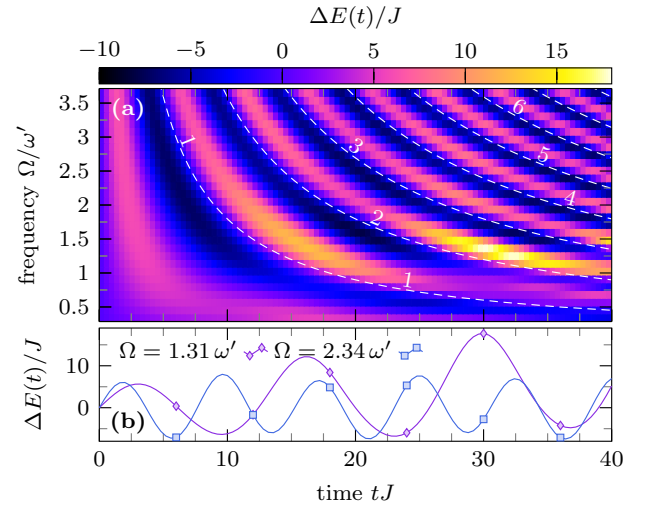


FIG. 5. (a) Energy difference $\Delta E(t) = E(t) - E(0)$ between initial time and t as a function of time t and driving frequency Ω . White dashed lines mark those times for which $t = 2\pi n/\Omega$. (b) Cut along constant Ω -lines as indicated. Parameters are $M = 64$, $N = 32$, $V_0 = 0.01 J$, $\delta V = 0.002 J$ and $U = 8 J$.

driving, the energy oscillates with the frequency Ω and with small variations in the amplitudes.

Effective site-dependent hopping – The parametric driving of the global trap can also be used to create a spatially varying hopping strength. By a time-dependent unitary transformation, the time dependence of the potential can be converted to a time- and site-dependent hopping amplitude $J_\ell(t) = J \sum_m \mathcal{J}_m(\delta V[\ell - \ell_0]/\Omega) e^{-im\Omega t}$ with the m -th Bessel function of first kind $\mathcal{J}_m(x)$. Thus, for large enough driving frequency Ω the time average yields an effective local hopping $J_{\text{eff}} = J \mathcal{J}_0(\delta V[\ell - \ell_0]/\Omega)$, where the spatial dependence is imprinted by the Bessel function $\mathcal{J}_0(x)$.

Conclusions – We have analyzed the parametric resonance condition for a driven one-dimensional Bose-Hubbard model with a periodically modulated harmonic trap. Combining a variational mean-field approach and a numerically exact treatment we have demonstrated that locating the onset of instability allows, in principle, to determine the atom interaction strength. Thus, dynamically probing a quantum many-body system with a periodic modulation of the harmonic confinement provides a novel diagnostic tool, which warrants an experimental realization in the realm of ultracold Bose gases.

Acknowledgements – This work was supported by the German Research Foundation (DFG), the DFG Collaborative Research Centers SFB 925 and SFB/TR185, and by the Academy of Finland (contract No. 275245).

-
- [1] M. Bukov, L. D'Alessio, and A. Polkovnikov, *Adv. Phys.* **64**, 139 (2015).
- [2] F. Schmitt, P.S. Kirchmann, U. Bovensiepen, R.G. Moore, L. Rettig, M. Krenz, J.-H. Chu, N. Ru, L. Perfetti, D.H. Lu, M. Wolf, I.R. Fisher, and Z.-X. Shen, *Science* **321**, 1649 (2008).
- [3] R. Yuzupov, T. Mertelj, V.V. Kabanov, S. Brazovskii, P. Kusar, J.-H. Chu, I.R. Fisher, and D. Mihailovic, *Nature Phys.* **6**, 681 (2010).
- [4] S. Hellmann, M. Beye, C. Sohrt, T. Rohwer, F. Sorgenfrei, H. Redlin, M. Källäne, M. Marczynski-Bühlrow, F. Hennies, M. Bauer, A. Föhlisch, L. Kipp, W. Wurth, and K. Rossnagel, *Phys. Rev. Lett.* **105**, 187401 (2010).
- [5] T. Rohwer, S. Hellmann, M. Wiesenmayer, C. Sohrt, A. Stange, B. Slomski, A. Carr, Y. Liu, L.M. Avila, M. Källäne, S. Mathias, L. Kipp, K. Rossnagel, and M. Bauer, *Nature* **471**, 490 (2011).
- [6] M. Rini, R. Tobey, N. Dean, J. Itatani, Y. Tomioka, Y. Tokura, R.W. Schoenlein, and A. Cavalleri, *Nature* **449**, 72 (2007).
- [7] D.J. Hilton, R.P. Prasankumar, S. Fourmaux, A. Cavalleri, D. Brassard, M.A. El Khakani, J.C. Kieffer, A.J. Taylor, and R.D. Averitt, *Phys. Rev. Lett.* **99**, 226401 (2007).
- [8] M. Liu, H.Y. Hwang, H. Tao, A.C. Strikwerda, K. Fan, G.R. Keiser, A.J. Sternbach, K.G. West, S. Kittiwatanakul, J. Lu, S.A. Wolf, F.G. Omenetto, X. Zhang, K. A. Nelson, and R.D. Averitt, *Nature* **487**, 345 (2012).
- [9] J. Demsar, R.D. Averitt, A.J. Taylor, V.V. Kabanov, W.N. Kang, H.J. Kim, E.M. Choi, and S.I. Lee, *Phys. Rev. Lett.* **91**, 267002 (2003).
- [10] J. Graf, C. Jozwiak, C.L. Smallwood, H. Eisaki, R.A. Kaindl, D.-H. Lee, and A. Lanzara, *Nature Phys.* **7**, 805 (2011).
- [11] C.L. Smallwood, J.P. Hinton, C. Jozwiak, W. Zhang, J.D. Koralek, H. Eisaki, D.-H. Lee, J. Orenstein, and A. Lanzara, *Science* **336**, 1137 (2012).
- [12] R. Matsunaga, Y.I. Hamada, K. Makise, Y. Uzawa, H. Terai, Z. Wang, and R. Shimano, *Phys. Rev. Lett.* **111**, 057002 (2013).
- [13] D. Fausti, R.I. Tobey, N. Dean, S. Kaiser, A. Dienst, M.C. Hoffmann, S. Pyon, T. Takayama, H. Takagi, and A. Cavalleri, *Science* **331**, 189 (2011).
- [14] R. Mankowsky, A. Subedi, M. Först, S.O. Mariager, M. Chollet, H.T. Lemke, J.S. Robinson, J.M. Glownia, M.P. Minitti, A. Frano, M. Fechner, N.A. Spaldin, T. Loew, B. Keimer, A. Georges, and A. Cavalleri, *Nature* **516**, 71 (2014).
- [15] W. Hu, S. Kaiser, D. Nicoletti, C.R. Hunt, I. Gierz, M.C. Hoffmann, M. Le Tacon, T. Loew, B. Keimer, and A. Cavalleri, *Nature Mater.* **13**, 705 (2014).
- [16] S. Kaiser, C.R. Hunt, D. Nicoletti, W. Hu, I. Gierz, H.Y. Liu, M. Le Tacon, T. Loew, D. Haug, B. Keimer, and A. Cavalleri, *Phys. Rev. B* **89**, 184516 (2014).
- [17] M. Först, A.D. Caviglia, R. Scherwitzl, R. Mankowsky, P. Zubko, V. Khanna, H. Bromberger, S.B. Wilkins, Y.-D. Chuang, W.S. Lee, W.F. Schlotter, J.J. Turner, G.L. Dakovski, M.P. Minitti, J. Robinson, S.R. Clark, D. Jaksch, J.-M. Triscone, J.P. Hill, S.S. Dhesi, and A. Cavalleri, *Nature Mater.* **14**, 883 (2015).
- [18] R. Singla, G. Cotugno, S. Kaiser, M. Först, M. Mitrano, H.Y. Liu, A. Cartella, C. Manzoni, H. Okamoto, T. Hasegawa, S.R. Clark, D. Jaksch, and A. Cavalleri, *Phys. Rev. Lett.* **115**, 187401 (2015).
- [19] M. Mitrano, A. Cantaluppi, D. Nicoletti, S. Kaiser, A. Perucchi, S. Lupi, P. Di Pietro, D. Pontiroli, M. Ricco, A. Subedi, S. R. Clark, D. Jaksch, and A. Cavalleri, *Nature* **530**, 461 (2016).
- [20] R. Citro, E.G.D. Torre, L. D'Alessio, A. Polkovnikov, M. Babadi, T. Oka, and E. Demler, *Ann. Phys. (New York)* **360**, 694 (2015).
- [21] C. Zerbe and P. Hänggi, *Phys. Rev. E* **52**, 1533 (1995).
- [22] M. Thorwart, P. Reimann, and P. Hänggi, *Phys. Rev. E* **62**, 5808 (2000).
- [23] A. Polkovnikov, K. Sengupta, A. Silva, and M. Vengalattore, *Rev. Mod. Phys.* **83**, 863 (2011).
- [24] P. Törmä and K. Sengstock (Eds), *Ultrafast Dynamics of Quantum Systems: Physical Processes and Spectroscopic Techniques*, Imperial College Press, 2014.
- [25] T. Langen, R. Geiger, and J. Schmiedmayer, *Ann. Rev. Cond. Mat. Phys.* **6**, 201 (2015).
- [26] J. Eisert, M. Friesdorf, and C. Gogolin, *Nature Phys.* **11**, 124 (2015).
- [27] H. Saito, and M. Ueda, *Phys. Rev. Lett.* **90**, 040403 (2003).
- [28] S.E. Pollack, D. Dries, M. Junker, Y. P. Chen, T. A. Corcovilos, and R.G. Hulet, *Phys. Rev. Lett.* **102**, 090402 (2009).
- [29] W. Cairncross and A. Pelster, *Europ. Phys. J. D* **68**, 106 (2014).
- [30] A. Eckardt and M. Holthaus, *Phys. Rev. Lett.* **101**, 245302 (2008).
- [31] A. Zenesini, H. Lignier, D. Ciampini, O. Morsch, and E. Arimondo, *Phys. Rev. Lett.* **102**, 100403 (2009).
- [32] A. Rapp, X. Deng, and L. Santos, *Phys. Rev. Lett.* **109**, 203005 (2012).
- [33] T. Wang, X.-F. Zhang, F.E.A. dos Santos, S. Eggert, and A. Pelster, *Phys. Rev. A* **90**, 013633 (2014).
- [34] N. Goldman, and J. Dalibard, *Phys. Rex. X* **4**, 031027 (2014).
- [35] M. Holthaus, *J. Phys. B: At. Mol. Opt. Phys* **49**, 013001 (2016).
- [36] A. Eckardt, eprint [arXiv:1606.08041](https://arxiv.org/abs/1606.08041), *Rev. Mod. Phys.* (in press).
- [37] G. Tang, S. Eggert, and A. Pelster, *New J. Phys.* **17**, 123016 (2015).
- [38] C. Sträter, S.C.L. Srivastava, and A. Eckardt, *Phys. Rev. Lett.* **117**, 205303 (2016).
- [39] H. Lignier, C. Sias, D. Ciampini, Y. Singh, A. Zenesini, O. Morsch, and E. Arimondo, *Phys. Rev. Lett.* **99**, 220403 (2007).
- [40] J. Struck, C. Ölschläger, R. Le Targat, P. Soltan-Panahi, A. Eckardt, M. Lewenstein, P. Windpassinger, and K. Sengstock, *Science* **333**, 996 (2011).
- [41] J. Struck, C. Ölschläger, M. Weinberg, P. Hauke, J. Simonet, A. Eckardt, M. Lewenstein, K. Sengstock, and P. Windpassinger, *Phys. Rev. Lett.* **108**, 225304 (2012).
- [42] F. Meinert, M. J. Mark, K. Lauber, A.J. Daley, and H.-C. Nägerl, *Phys. Rev. Lett.* **116**, 205301 (2016).
- [43] N. Goldman, J.C. Budich, and P. Zoller, *Nature Phys.* **12**, 639 (2016).
- [44] L. D'Alessio and A. Polkovnikov, *Ann. Phys. (New York)* **333**, 854 (2013).
- [45] T. Kuwahara, T. Mori, and K. Saito, *Ann. Phys. (New*

- York) **367**, 96 (2016).
- [46] V.M. Pérez-García, H. Michinel, J.I. Cirac, M. Lewenstein, and P. Zoller, Phys. Rev. Lett. **77**, 5320 (1996).
 - [47] S. M. Forghani and T. G. Ritto, Nonl. Dyn. **86**, 1561 (2016).
 - [48] See Supplemental Material at [URL will be inserted by publisher] for calculational details.
 - [49] G. Vidal, Phys. Rev. Lett. **91**, 147902 (2003).
 - [50] G. Vidal, Phys. Rev. Lett. **93**, 040502 (2004).
 - [51] A. J. Daley, C. Kollath, U. Schollwöck, and G. Vidal, J. Stat. Mech.: Theor. Exp. (**2004**), P04005.
 - [52] Note that the distribution of the site occupation number $\langle n_\ell \rangle$ is no longer Gaussian.
 - [53] T. D. Kühner and H. Monien, Phys. Rev. B **58**, R14741 (1998).
 - [54] F. E. A. dos Santos and A. Pelster, Phys. Rev. A **79**, 013614 (2009).